J Mater Sci (2011) 46:4243–4247
DOI 10.1007/s10853-011-5257-6

IIB 2010

# First measurement of the heat effect of the grain boundary wetting phase transition

**B. B. Straumal · O. A. Kogtenkova · S. G. Protasova · P. Zięba · T. Czeppe · B. Baretzky · R. Z. Valiev**

Received: 28 August 2010 / Accepted: 6 January 2011 / Published online: 19 January 2011


**Abstract** The melting of coarse- and fine-grained Al–Zn–Mg alloys was studied by the differential scanning calorimetry. The asymmetric shape of the melting curve indicates the heat effect of the grain boundaries (GBs) wetting. The difference between melting heat of coarse- and fine-grained samples permitted to estimate the GB wetting heat effect per GB unit area. It is $\sim 0.15$ J/m$^2$ for the Al–5 wt% Zn–2 wt% Mg alloy and $\sim 1$ J/m$^2$ for the Al–10 wt% Zn–4 wt% Mg alloy.

## Introduction

The wetting of grain boundaries (GBs) by a liquid phase (melt) plays an important role in the materials science. It is crucial for the liquid phase sintering, soldering, brazing, precise casting, and other processes. The GB is completely wetted if the contact angle between GB and melt is zero. In this case, the liquid phase has to substitute the GB separating both grains. The GB is incompletely wetted if the contact angle between GB and the melt is finite. In this case, the GB can exist in the equilibrium contact with the liquid phase. Cahn [1] and Ebner and Saam [2] first assumed that the (reversible) transition from the incomplete to the complete wetting can proceed with increasing temperature, and it is a true surface phase transformation. The transition from the incomplete to the complete GB wetting can be observed if the energy of two solid–liquid interfaces 2 $\sigma_{SL}$ reduces to lower than the GB energy $\sigma_{GB} > 2\ \sigma_{SL}$. Cahn's idea [1] was the "driving force" for the experimental finding of GB wetting phase transformations, initially made in the Zn–Sn, Zn–Sn–Pb, and Ag–Pb polycrystals [3, 4]. At a later state, the original experimental data were reconsidered from this point-of-view, and numerous indications on the GB wetting phase transformations were found, particularly for the Zn–Sn, Al–Cd, Al–In, Al–Pb [5] and W–Ni, W–Cu, W–Fe, Mo–Ni, Mo–Cu, Mo–Fe [6] polycrystals. The first exact measurements of the temperature dependence for the contact angle with the melt were made using the individual GBs in the specially grown bicrystals in the Cu–In [7], Al–Sn [8], and Zn–Sn [9] systems.

The substitution of a GB by a liquid layer leads to the heat release equal to ($\sigma_{GB}$–2 $\sigma_{SL}$). However, to the best of the knowledge, the heat effect of a GB wetting phase transition has been never measured before. The most direct way to measure the heat effect of a GB wetting transition is to compare the values of the melting heat for the coarse-grained and fine-grained polycrystals of an alloy where all GBs become completely wetted between solidus and liquidus temperatures. The Al–5 wt% Zn–2 wt% Mg and Al–10 wt% Zn–4 wt% Mg ternary alloys are the good candidates for such measurements. It was observed earlier

B. B. Straumal (✉) · O. A. Kogtenkova · S. G. Protasova
Institute of Solid State Physics, Russian Academy of Sciences, Chernogolovka 142432, Russia
e-mail: straumal@issp.ac.ru; straumal@mf.mpg.de

B. B. Straumal · S. G. Protasova
Max-Planck Institut für Metallforschung, Heisenbergstrasse 3, 70569 Stuttgart, Germany

P. Zięba · T. Czeppe
Institute of Metallurgy and Materials Science, Polish Academy of Sciences, Reymonta St. 25, 30-059 Cracow, Poland

B. B. Straumal · B. Baretzky
Karlsruher Institut für Technologie (KIT), Institut für Nanotechnologie, Hermann-von-Helmholtz-Platz 1, 76344 Eggenstein-Leopoldshafen, Germany

R. Z. Valiev
Ufa State Aviation Technical University, Ufa 450000, Russia

that all boundaries between grains of the Al-based solid solution (Al) become completely wetted about 37 °C below the liquidus temperature of the Al–10 wt% Zn–4 wt% Mg alloy and about 60 °C below the liquidus temperature of the Al–5 wt% Zn–2 wt% Mg alloy [10]. The fine-grained structure in both alloys can be obtained using the severe plastic deformation [11, 12].

## Experimental

The Al–5 wt% Zn–2 wt% Mg and Al–10 wt% Zn–4 wt% Mg alloys were prepared of the high purity components (5N5 Al, 5N Zn and 4N5 Mg) by the vacuum induction melting. As-cast disks of these alloys obtained after grinding, sawing and chemical etching were subjected to the high pressure torsion (HPT) at room temperature under the pressure of 5 GPa in a Bridgman anvil type unit (5 torsions, duration of process about 300 s) [13]. Transmission electron microscopy (TEM) investigations of the as-cast coarse-grained (CG) and fine-grained HPT-samples have been carried out in a JEM–4000FX microscope at an accelerating voltage of 400 kV. Both the as-cast CG and fine-grained HPT-samples were studied with the aid of differential scanning calorimetry (DSC) using the TA Instruments calorimeters (models 910 and 1600) in the dry nitrogen atmosphere at the cooling and heating rates of 10 K/min. The heating rate of 10 K/min has been chosen because at the higher heating rate of 20 K/min the effects, which the authors would like to study became less visible. The lower heating rates of 5 or 1 K/min led to the substantial grain growth in the HPT-treated samples, and we lost too much grain boundaries. In order to record the DSC curves, the samples were heated from 20 to 670 °C. However, the heating in calorimeter led to the grain growth in the HPT samples. In order to know the grain size in the sample before the start of the wetting transition, the separate HPT samples were heated in the DSC chamber up to the 320 °C and then cooled down to the room temperature in the flow of dry nitrogen. The TEM measurements of the grain size have been carried out in a PHILIPS CM 20 microscope at an accelerating voltage of 400 kV. The temperature 320 °C has been chosen because it is very close to the solidus line. Therefore, the structure of the samples heated up in the DSC chamber to the 320 °C and then quenched to the room temperature allowed to estimate the grain size in the HPT samples continuously heated 20 to 670 °C just before the beginning of their melting.

## Results and discussion

The coarse grained alloys (state before HPT deformation) contained two phases. The majority phase was the supersaturated (Al) solid solution with grain size about 500 μm and almost dislocation-free with a dislocation density of about $10^{10}$ $m^{-2}$. The minority phase in the Al–10 wt% Zn–4 wt% Mg alloy was τ-phase ($Mg_{32}(ZnAl)_{39}$). It formed colonies with a size about 500 nm. However, the X-rays diffraction did not reveal the presence of τ-phase in the alloys, which means that its volume fraction is less than 1% [12]. After HPT, both Al–Zn–Mg alloys contain (Al) grains with the size of ∼150 nm. Selected area diffraction patterns revealed also the presence of τ-phase particles. They are uniformly distributed in the material and have a size of about 10 nm. Also in deformed alloys X-ray analysis did not detect the τ-phase in both alloys. It means that its volume fraction is low. After heating in the DSC chamber up to the 320 °C, the grain size of as-cast alloys did not increase significantly and remained about 500 μm. The grain size in the HPT-treated Al–10 wt% Zn–4 wt% Mg alloy increased to about 600 nm (Fig. 1b). The grain size in the HPT-treated Al–5 wt% Zn–2 wt% Mg alloy increased to 10 μm (Fig. 1a). The microstructure shown in

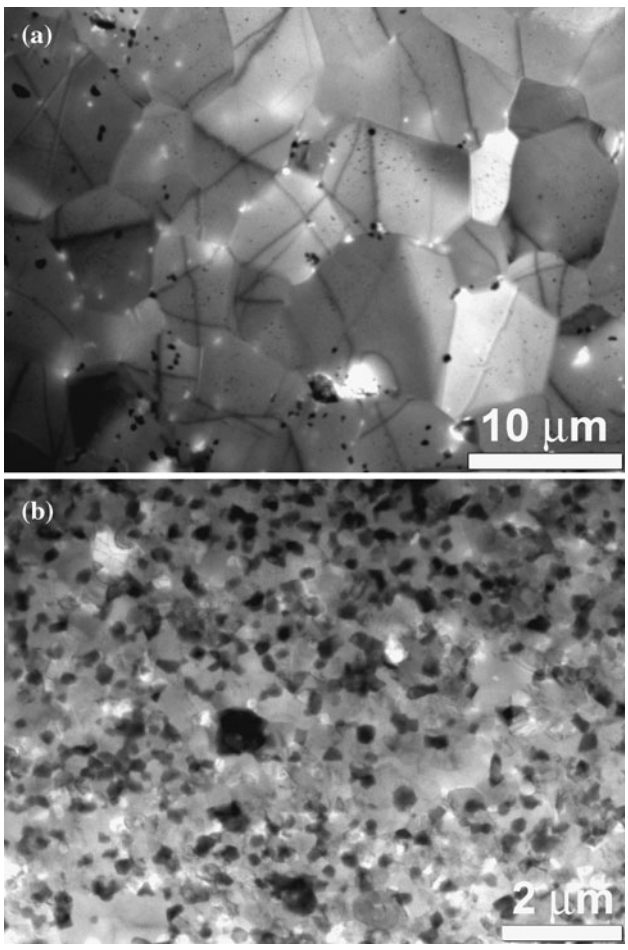


**Fig. 1** TEM micrographs of the **a** Al–10 wt% Zn–4 wt% Mg and **b** Al–5 wt% Zn–2 wt% Mg alloys after HPT and subsequent heating up to 320 °C in DSC chamber

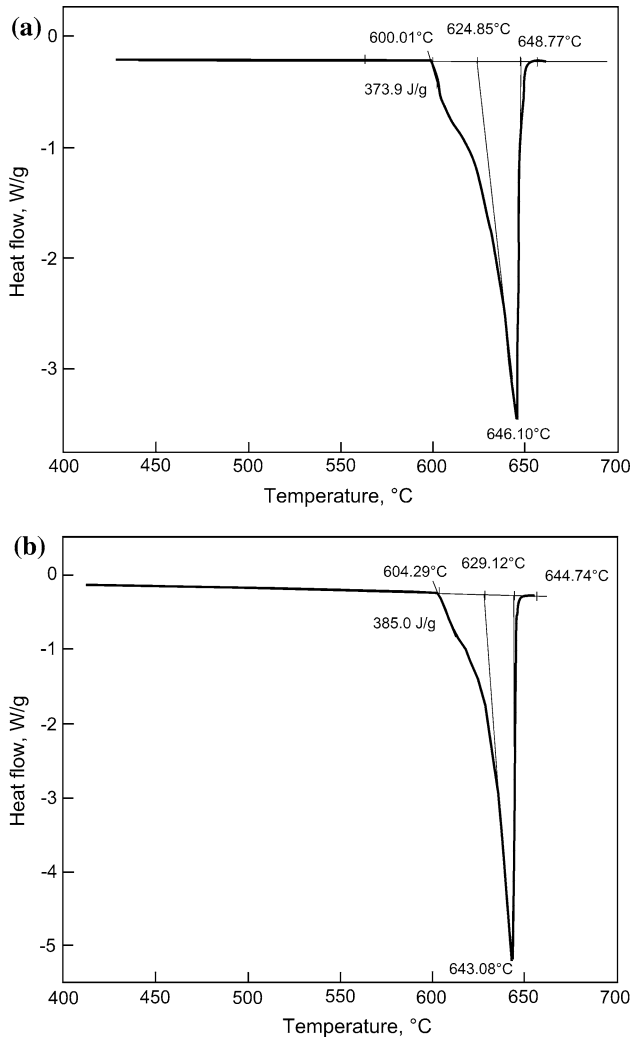


**Fig. 2** Temperature dependence of heat flow (DSC curve) for the Al–5 wt% Zn–2 wt% Mg alloys for the **a** as-cast coarse-grained (grain size 500 μm) and **b** fine-grained samples after HPT (initial grain size 150 nm, grain size after subsequent heating up to 320 °C in DSC chamber 10 μm)

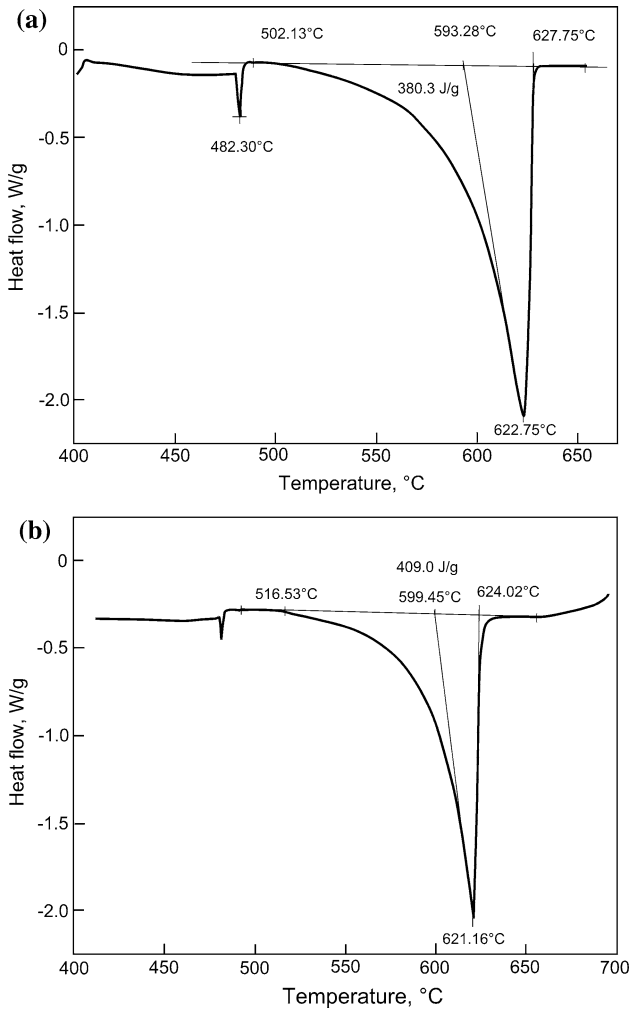


**Fig. 3** Temperature dependence of heat flow (DSC curve) for the Al–10 wt% Zn–4 wt% Mg alloys for the **a** as-cast coarse-grained (grain size 500 μm) and **b** fine-grained samples after HPT (initial grain size 150 nm, grain size after subsequent heating up to 320 °C in DSC chamber 600 nm)

Fig. 1 was the starting point for the high-temperature DSC experiments. It is completely recrystallized, the higher elastic energy stored in the HPT-processed samples as compared to the as-cast almost dislocation-free samples fully relaxed after heating. The only remained difference is the smaller grain size of HPT-samples.

In Fig. 2, temperature dependences of heat flow (DSC curves) are shown for the Al–5 wt% Zn–2 wt% Mg alloys heated from 20 to 670 °C with the rate of 10 K/min. Only the high-temperature part between 400 and 670 °C is shown in Fig. 2. Two curves present the results for the as-cast coarse-grained samples with the grain size about 500 μm (Fig. 2a) and for the fine-grained samples after HPT (Fig. 2b). The grain size immediately after HPT was about 150 nm. The grain size after subsequent heating up to 320 °C in DSC chamber was 10 μm. The integral heat effect of the melting was 373.9 J/g for the CG-sample and 385.0 J/g for the fine-grained sample.

In Fig. 3, the similar DSC curves are shown for the Al–10 wt% Zn–4 wt% Mg alloys. The grain size immediately after HPT was about 120 nm. The grain size after subsequent heating up to 320 °C in DSC chamber was 600 nm. The integral heat effect of the melting was 380.3 J/g for the CG-sample and 409.0 J/g for the fine-grained sample. Small sharp minimum at ~482 °C (below the start of the melting) corresponds most probably to the dilution of particles of the τ-phase. The obtained values of the melting heat effect for the coarse-grained samples are between those known from the literature for the pure aluminum 399.9 ± 1.3 J/g [14], 401.3 ± 1.6 J/g [15] and for the alloy with higher content of zinc and magnesium (Al–34 wt% Mg–6 wt% Zn, 329 J/g [16]).

According to the standard approach to the quantification of DSC curves of the alloys melting between solidus and liquidus temperatures [17] (these procedures are also included in the quantification software of modern DSC equipment), the position of a deep minimum corresponds to the end of melting, i.e., to the liquidus temperature. The measured minimum positions for both samples are in a good compliance with the literature data for the liquidus in the Al–Zn–Mg bulk phase diagram obtained in [18] by the linear interpolation of liquidus lines from [19] and experimentally in [10]. In the standard case [17], the left side of the DSC minima for the melting follows the linear tangent almost until the intersection point with the base line. In this case (Figs. 2, 3), each of DSC curves deviates from this tangential. The temperatures given by the conventional procedure (i.e., defined using the intersection of the base-line and the tangential to the left side of the minimum) lie deep in the middle between solidus and liqiudus lines [10, 18]. A kind of broad "shoulder" is visible in the left part of each melting minimum. Even more, the presence of a secondary, superimposed, peak (itself with a minimum) may be guessed from the Figs. 2 and 3 for both as-cast coarse-grained and fine-grained HPT-samples. Such "shoulder" is more visible in Fig. 2. These "shoulders" positions to the left of the main DSC minimum reveal the second weak melting process in the samples. It is possible to draw the second tangential at the lower temperature in comparison with the "main" melting tangential (Figs. 2, 3). The temperatures obtained by the intersection of second tangential with a base line are now close to the values of solidus temperatures [10, 18].

It was supposed that this two-stage melting is due to the transition from incomplete to complete wetting of GBs by the melt. Such transition was observed both in binary Al–Zn, Al–Mg, and ternary Al–Zn–Mg alloys [10, 18, 20, 21]. During conventional melting, the bulk phase gradually becomes liquid between solidus and liquidus lines. In this case, the tangential to the left side of the DSC melting curve intersects the base line almost in the point where the DSC melting curve starts to come down from the base line. In case of GB wetting, the first portions of melted bulk redistribute along GBs in order to wet them and to separate the remaining solid grain one from another. The heat of the melting also redistributes to the lower temperatures, the shape of the DSC melting curve changes, and the tangential shifts to the higher temperature from the bulk solidus (Figs 2 and 3). This shift is more pronounced in the HPT samples with smaller grains (4 K in Fig. 2 and 6 K in Fig. 3). The shape change of the DSC curve depends on the GB energy spectrum and, therefore, on the spectrum of GB wetting temperatures $T_w$. In the extreme case, if the $T_w$ temperatures group close to the solidus point, the "shoulder" in melting curve is rather pronounced (like in Fig. 2). If the $T_w$ temperatures are uniformly distributed, the "shoulder" in melting curve is less pronounced (Fig. 3), and only the shift of the tangential with the base line indicates the GB melting effect.

The value of the melting heat is also slightly different in the coarse-grained and fine-grained samples. The melting heat effect in both studied alloys was higher in case of fine-grained samples. Knowing the difference in the heat effect and difference in the grain size, one can roughly estimate the additional heat effect for the unit area of GBs. In the Al–5 wt% Zn–2 wt% Mg alloy the heat effect is 373.9 J/g for the CG samples and 385.0 J/g for the HPT samples. If heat difference on the difference of the GB area per 1 g was divided, the authors would get about 0.15 J/m$^2$. In the Al–10 wt% Zn–4 wt% Mg alloy, the heat effect is 380 J/g for the CG samples and 409 J/g for the HPT samples. After division of this difference on the difference of the GB area per 1 g, the value of 1 J/m$^2$ was obtained. The lowest possible GB energy in Al and Al-based alloys is the free energy of symmetric twin GBs (in other words, the free energy of a stacking fault). In pure Al it is about 0.166 J/m$^2$ [22, 23]. The free energy of a stacking fault decreases by the Al alloying with Mg, it is 0.110 J/m$^2$ for the Al–0.7 wt% Mg alloy [24]. As it can be expected, the heat effect for the unit GB area in these alloys is higher than the value for the stacking fault free energy. The higher heat effect of a GB wetting in the Al–10 wt% Zn–4 wt% Mg alloy corresponds also to the much broader "shoulder" on the left side of the DSC melting curve. The difference in the GB heat effect may be due to the difference in the GB misorientation spectra (called also as GB character distribution [25–27]) in two alloys. This effect should be studied in the future using the electron-backscattering diffraction (EBSD) [25–27].

It can be concluded that the transition from incomplete to complete GB wetting in ternary Al–Zn–Mg alloys reflected itself in the asymmetric shape of the melting curve. The difference between melting heat of coarse- and fine-grained samples permitted to estimate for the first time the GB wetting heat effect per GB unit area. The observed effect means that the more detailed investigations are desired to be done for the investigations of the GB wetting thermal effect. For example, the careful check of the change of grain structure has to be performed just below and just above the solidus as well as close to the "shoulder" position between solidus and liquidus lines. The evolution of the GB character distribution during a DSC experiment has to be studied by EBSD, as well as its influence on the wetting thermal effect. And the last but not least, the reversibility of the thermal effect of GB wetting has to be studied as well.

**Acknowledgements** Authors thank the Russian Foundation for Basic Research (contract 09-02-90406) and the Ukrainian Fundamental Research State Fund (grant no. X28.7049) for the financial support. Authors cordially thank Prof. E. Rabkin and Dr. A. Gornakova for stimulating discussions.

## References

1. Cahn JW (1977) J Chem Phys 66:3667
2. Ebner C, Saam WF (1977) Phys Rev Lett 38:1486
3. Passerone A, Eustathopoulos N, Desré P (1977) J Less Common Met 52:37
4. Passerone A, Sangiorgi R, Eustathopoulos N (1982) Scr metall 16:547
5. Eustathopoulos N (1983) Int Met Rev 28:189
6. Straumal BB (2003) Grain boundary phase transitions. Nauka publishers, Moscow in Russian
7. Straumal B, Muschik T, Gust W et al (1992) Acta Metall Mater 40:939
8. Straumal B, Molodov D, Gust W (1995) Interface Sci 3:127
9. Straumal B, Gust W, Watanabe T (1999) Mater Sci Forum 294–296:411
10. Straumal BB, Kogtenkova O, Zięba P (2008) Acta Mater 56:925
11. Straumal BB, Baretzky B, Mazilkin AA et al (2004) Acta Mater 52:4469
12. Mazilkin AA, Kogtenkova OA, Straumal BB et al (2005) Def Diff Forum 237–240:739
13. Valiev RZ, Islamgaliev RK, Alexandrov IV (2000) Prog Mater Sci 45:103
14. Stølen S, Grønvold F (1999) Thermochim Acta 327:1
15. Della Gatta G, Richardson M, Sarge SM et al (2006) Pure Appl Chem 78:1455
16. Sun JQ, Zhang RY, Liu ZP et al (2007) Energy Convers Manag 48:619
17. Dean JA (1995) The analytical chemistry handbook. McGraw Hill, New York (Standards ASTM D 3417, ASTM D 3418, ASTM E 1356, ISO 11357)
18. Straumal B, Valiev R, Kogtenkova O et al (2008) Acta Mater 56:6123
19. Massalski TB (ed) (1990) Binary alloy phase diagrams. ASM International, Materials Park
20. Straumal B, López G, Gust W et al (2004) In: Zehetbauer MJ, Valiev RZ (eds) Nanomaterials by severe plastic deformation: fundamentals, processing, applications. John Wiley, VCH, Weinheim
21. Straumal BB, López G, Mittemeijer EJ et al (2003) Def Diff Forum 216–217:307
22. Cottrell AH (1958) Trans AIME 212:192
23. Mullins WW (1956) Acta Metal 4:421
24. Talbot J (1963) Recovery and Recrystallization of Metals. Wiley Interscience, New York
25. Kobayashi S, Tsurekawa S, Watanabe T et al (2010) Scr Mater 62:294
26. Tsurekawa S, Okamoto K, Kawahara K et al (2005) J Mater Sci 40:895. doi:10.1007/s10853-005-6507-2
27. Downey ST II, Bembridge N, Kalu PN et al (2007) J Mater Sci 42:9543. doi:10.1007/s10853-007-1959-1